REPORT DOCUMENTATION PAGE

Form Approved
OMB No. 0704-0188

1. AGENCY USE ONLY *(Leave blank)*	2. REPORT DATE	3. REPORT TYPE AND DATES COVERED
	January 11, 1999	Technical Report # 46

4. TITLE AND SUBTITLE
X-ray Crystal Structures and Photophysical Properties of New Conjugated Oligoquinolines

5. FUNDING NUMBERS
N00014-94-1-0540
Kenneth J. Wynne
R & T Code 3132111

6. AUTHOR(S)
Samson A. Jenekhe, Ashok S. Shetty, Elizabeth B. Liu, and Rene J. Lachicotte

7. PERFORMING ORGANIZATION NAMES(S) AND ADDRESS(ES)
University of Rochester
Department of Chemical Engineering
206 Gavett hall, Box 270166
Rochester. NY 14627-0166

8. PERFORMING ORGANIZATION REPORT NUMBER
46

9. SPONSORING / MONITORING AGENCY NAMES(S) AND ADDRESS(ES)
Office of Naval Research
800 North Quincy Street
Arlington, VA 22217-5000

10. SPONSORING / MONITORING AGENCY REPORT NUMBER

11. SUPPLEMENTARY NOTES
Submitted for publication in CHEMISTRY OF MATERIALS.

a. DISTRIBUTION / AVAILABILITY STATEMENT
Reproduction in whole or in part is permitted for any purpose of the United States Government. This document has been approved for public release and sale; its distribution is unlimited.

12. DISTRIBUTION CODE

13. ABSTRACT *(Maximum 200 words)*

The synthesis, characterization, X-ray crystal structures, and photophysical properties of two conjugated oligoquinolines, 2,2'-bis(4-phenylquinoline)-1,4-phenylene (**2a**) and 2,2'-bis(4-phenylquinoline)-4,4'-biphenylene (**2b**), are reported. Both **2a** and **2b** crystallized in a monoclinic lattice with different unit cell parameters and space groups. The X-ray crystal structures reveal that **2a** exhibits intermolecular face-to-face π-π stacking whereas **2b** manifests edge-to-face π-π stacking. The dilute solution and solid state optical absorption and emission spectra of **2b** were red-shifted from those of **2a** because of the greater degrees of π-electron delocalization and intramolecular charge transfer in **2b** compared to **2a**. The strongly Stokes shifted solid state emission bands of both oligomers from their absorption bands are attributed to excimer formation. These conjugated oligoquinolines with known X-ray crystal structures are excellent model systems for elucidating the structure and properties of polyquinolines and may also find device applications as n-type semiconductors.

14. SUBJECT TERMS
Oligoquinolines; conjugated oligomers; X-ray crystal structures; π-stacking; photophysics; n-type semiconductors.

15. NUMBER OF PAGES
39

16. PRICE CODE

17. SECURITY CLASSIFICATION OF REPORT	18. SECURITY CLASSIFICATION OF THIS PAGE	19. SECURITY CLASSIFICATION OF ABSTRACT	20. LIMITATION OF ABSTRACT
Unclassified	Unclassified	Unclassified	Unlimited

OFFICE OF NAVAL RESEARCH

GRANT NO: N00014-94-1-0540

R&T Code 3132111
Kenneth J. Wynne

Technical Report NO. 46

X-ray Crystal Structures and Photophysical Properties of New Conjugated Oligoquinolines

By

Samson A. Jenekhe, Ashok S. Shetty, Elizabeth B. Liu, and Rene J. Lachicotte
Submitted for Publication

In

CHEMISTRY OF MATERIALS

Departments of Chemical Engineering
and Chemistry
University of Rochester, New York 14627

January 11, 1999

X-ray Crystal Structures and Photophysical Properties of New Conjugated Oligoquinolines.

Ashok S. Shetty,[†] Elizabeth B. Liu,[†] Rene J. Lachicotte,[§] and Samson A. Jenekhe*[,†,§]
Departments of Chemical Engineering and Chemistry and Center for Photoinduced Charge Transfer, University of Rochester, Rochester, New York 14627-0166.

Abstract

The synthesis, characterization, X-ray crystal structures, and photophysical properties of two conjugated oligoquinolines, 2,2'-bis(4-phenylquinoline)-1,4-phenylene (**2a**) and 2,2'-bis(4-phenylquinoline)-4,4'-biphenylene (**2b**), are reported. Both **2a** and **2b** crystallized in a monoclinic lattice with different unit cell parameters and space groups. The X-ray crystal structures reveal that **2a** exhibits intermolecular face-to-face π-π stacking whereas **2b** manifests edge-to-face π-π stacking. The dilute solution and solid state optical absorption and emission spectra of **2b** were red-shifted from those of **2a** because of the greater degrees of π-electron delocalization and intramolecular charge transfer in **2b** compared to **2a**. The strongly Stokes shifted solid state emission bands of both oligomers from their absorption bands are attributed to excimer formation. These conjugated oligoquinolines with known X-ray crystal structures are excellent model systems for elucidating the structure and properties of polyquinolines and may also find device applications as n-type semiconductors.

[†] Department of Chemical Engineering and Center for Photoinduced Charge Transfer.
[§] Department of Chemistry.

X-ray Crystal Structures and Photophysical Properties of New Conjugated Oligoquinolines.

Ashok S. Shetty,[†] Elizabeth B. Liu,[†] Rene J. Lachicotte,[§] and Samson A. Jenekhe*[,†,§]
Departments of Chemical Engineering and Chemistry and Center for Photoinduced Charge Transfer, University of Rochester, Rochester, New York 14627-0166.

The synthesis, electronic structure, and optical, nonlinear optical and charge transport properties of numerous conjugated oligomers [1a] of polyenes,[1b] acenes,[1b] thiophene,[1c] pyrrole,[1d] *p*-phenylene,[1b] and *p*-phenylene vinylene [1a, 2] have been extensively investigated both as p-type (hole transport) organic semiconductors *per se* and as structurally well-defined model systems for the corresponding conjugated polymers.[1a] Few, if any, oligomers of n-type (electron transport) conjugated polymers such as the polyquinolines are known.[3-9] We report herein the synthesis, single crystal X-ray structures, and the photophysical properties of two new conjugated oligoquinolines. The oligomers are promising model systems for elucidating the structure-property relationships of conjugated polyquinolines and may also be useful as n-type semiconductors for device applications.

n-Type conjugated polymers by virtue of their electron transport, high electron affinity and interesting photophysical properties are of growing interest in electronic and optoelectronic devices. Polyquinolines, in particular, with the general structure **1** are high temperature conjugated polymers and possess interesting mechanical,[3] photoresponsive and photoconductive,[4] electron transport, [5, 6, 7] third-order nonlinear optical,[8,] and

[†] Department of Chemical Engineering and Center for Photoinduced Charge Transfer.
[§] Department of Chemistry.

electroluminescent, [6,7] properties. They have thus been attracting considerable attention for their potential use in thin film electronic and optoelectronic devices.[6,7]

Although, over several dozen polyquinolines have been reported in the last two decades, only one preliminary report has discussed the crystal structure of a rigid-rod polyquinoline, poly[2,2'-(p,p'-biphenylene)-6,6-bis(4-phenylquinoline)] (**1b**, PBPQ).[9] The study concluded that X-ray diffraction pattern of fibers spun from anisotropic solutions of this polymer showed that parallel chains along the direction of the fiber axis stack in nearly coplanar sheets with the two pendant phenyl groups on the 4-position of the quinoline units pointing toward one another.[9] The close packing of the polymer chains was invoked to explain the poor solubility in organic solvents and the photophysical properties[4-8] of the polyquinolines. However, a more rigorous study of the crystal structure of the conjugated polyquinolines by using monodisperse oligomers as model systems has not been conducted.

We synthesized, characterized, obtained single crystal X-ray structures, and investigated the photophysical properties of 2,2'-bis(4-phenylquinoline)-1,4-phenylene (**2a**) and 2,2'-bis(4-phenylquinoline)-4,4'-biphenylene (**2b**) (Scheme 1). Oligoquinolines **2a** and **2b** were synthesized by the Friedlander coupling [10] of two equivalents of 2-amino benzophenone with one equivalent of 1,4-diacetylbenzene or 4,4'-diacetylbiphenylene, respectively.[11]

Single crystals of the oligomers suitable for X-ray structural determination were obtained from concentrated chloroform solutions (30 mg/mL). Whereas **2a** crystallized as clusters of needles, **2b** crystallized as clusters of overlapping irregularly shaped blocks. Laue symmetry revealed a monoclinic crystal system for both **2a** and **2b**. The unit cell

parameters of a = 13.9932(8) Å, b = 4.0104(2) Å, c = 21.6130(13) Å, and β = 96.0320(10) for **2a**, and of a = 11.4460(2) Å, b = 8.3789(2) Å, c = 15.8601(3) Å, and β = 105.9710(10) for **2b**, were based upon the least-squares refinement of three dimensional centroids of > 3000 reflections for each crystal. The space groups were assigned as $P2/c$ and $P2_1/c$, respectively for **2a** and **2b**, and the structures refined to final residuals of R_1 = 3.95% for **2a**, and R_1 = 4.52% for **2b**. Further experimental details of the data collection and structure refinement can be found in the supporting information.

The molecular structure and crystal packing of the two oligomers are shown in Figures 1 and 2, respectively. In the crystal of oligomer **2a**, the molecule is located on a crystallographic center of symmetry at the midpoint of the central *p*-phenylene ring. The molecule in the crystal of oligomer **2b** is located on a crystallographic center of symmetry at the midpoint of the central inter-ring bond. In both oligomers, the quinoline moieties are in a crystallographically imposed *anti*-orientation with respect to each other. This result is very different from the structure of **1b** inferred from X-ray diffration patterns of fibers.[9] The *p*-phenylene ring in **2a** is twisted 26° from the mean plane of the quinoline moieties. Although the central phenylenes in oligomer **2b** are coplanar, they are twisted 13° relative to the mean plane of the quinoline moieties. The phenyl groups appended onto the quinoline moieties in both oligomers, are twisted *ca.* 49° relative to the quinoline moieties.

The molecular packing of the oligomers, as shown in Figures 1C and 2C, are dramatically different. In the case of **2a** (Figure 1C), the molecules pack in columns exhibiting intermolecular *face-to-face* π stacking (sandwich-type) separated by *ca.* 4 Å.[12] The pendant phenyl groups pack in a way that precludes intercolumn π-stacking.

Oligomer **2b** (Figure 2C), packs is a more complex fashion. It is dominated by an intermolecular *edge-to-face* stacking between the pendant phenyl and the biphenylene rings and between the pendant phenyl and the quinoline moieties at an intermolecular distance of *ca.* 3.6Å. Careful examination of the crystal structure reveals that the pendant phenyl groups are engaged in π-stacking interactions with both the biphenylene and the quinoline moieties of **2b**.

Optical absorption and fluorescence spectra of **2a** and **2b** in solution (chloroform and formic acid) are shown in Figure 3. The absorption maxima of **2b**, with a biphenylene linkage, is red shifted from that of **2a** in both solvents (Figure 3). The absorption spectrum of **2a** in chloroform (Figure 3A) shows peaks at 280 and 342 nm whereas that of **2b** reveals peaks at 294 and 348 nm. In the case of **2a**, the lower energy band is only 60% in intensity of the peak at 280 nm. In the case of **2b**, however, the two absorption bands are nearly of comparable intensity. On changing the solvent to formic acid in which the quinoline moieties are protonated, the absorption spectra of these oligomers change significantly (Figure 3 B). For oligomer **2a**, the absorption peak is red shifted by 20 nm as compared to that in chloroform (from 342 to 362 nm) whereas **2b** exhibits a much larger red-shift of 32 nm in absorption λ_{max} (from 348 to 380 nm).

The emission spectra of the oligoquinolines show similar dependence on the size of the aromatic group that links the two quinoline moieties and the solvent environment. The emission spectrum of **2b** in chloroform (Figure 3A) is red shifted from the emission maxima of **2a** (370 nm) by 14 nm. A similar red shift of 14 nm was observed between the emission maxima of **2a** (436 nm) and **2b** (450 nm) in formic acid (Figure 3B). The emission maxima of both **2a** and **2b**, in formic acid, are red shifted by 66 nm compared to

those in chloroform. In addition, as can be seen in Figures 3A and 3B the emission bands of both oligomers in formic acid are broader and less structured than those in chloroform. The luminescence quantum yields (Φ) [13] of **2a** were 7.4 and 41% in chloroform and formic acid, respectively, whereas **2b** had a Φ of 54% in both solvents. Thus the oligomers have higher luminescence quantum efficiencies in formic acid than in chloroform while in the same solvent systems **2b** is much more efficient than **2a**.

The bathochromic shift of the optical absorption of **2b** compared to **2a** is due in part to the larger number of π-electrons and a greater degree of π-electron delocalization along the oligomer backbone. The greater degree of π -electron delocalization of **2b** is in accord with the crystal structures of oligomer **2b**. As discussed above, the central aromatic rings in oligomer **2b** (Figure 2A) are mutually coplanar and are twisted 13° from the quinoline moities whereas the phenylene ring in **2a** is twisted 26° (Figure 1A) from the quinoline moities, precluding an efficient π-electron delocalization. The observed photophysical properties also suggest the presence of intramolecular charge transfer (ICT) between the central phenylene rings as donor groups and the quinoline moieties as acceptors.[14] The ICT is greater in **2b** than in **2a** because biphenylene moiety is a stronger π-electron donor than the single phenylene group in **2a**. In formic acid, protonation of the quinoline moieties makes them stronger acceptors and thereby enhancing ICT which accounts for the large spectral red shifts compared to chloroform. These oligomer results confirm that the previously reported effects of protonation on electronic delocalization of the conjugated polyquinolines are intrinsic to their molecular structures (repeat units).[5]

Optical absorption and fluorescence spectra of thin films of **2a** and **2b**, spin casted onto fused silica substrates from chloroform solutions, were also measured. The absorption spectrum of **2a** shows peaks at 284 and 346 nm whereas that of **2b** reveals peaks at 296 and 352 nm (Figure 4). The solid state absorption spectra of 2a and 2b are thus very similar to the dilute chloroform solution results, suggesting that aggregation of oligomer molecule does not significantly modify the electronic ground state of the materials. Freshly cast films of both oligomers had a broad emission maxima at 420 nm. After 24 hours in ambient conditions **2a** film exhibited an emission maxima at 470 nm whereas **2b** film still showed one emission peak at 420 nm with a shoulder at *ca.* 470 nm. However on annealing the films at 70°C in a vacuum oven for 24 hours **2b** film exhibited an emission maxima at 515 nm, whereas the emission maxima of the **2a** film remained unchanged at 470 nm (Figure 4). Because the thin film annealing process for **2b** takes longer compared to that of **2a**, it may be implied that the packing mode of **2b** in the solid state is more complicated than that of **2a** as confirmed by the single crystal X-ray structures of these oligomers. Annealed films of **2a** and **2b** had estimated fluorescence quantum yields [13] of 20% and 43%, respectively, which are consistent with the results in solution. The **2a** and **2b** emission bands at 470 and 515 nm, respectively, are significantly red shifted (100-131nm) from their corresponding emission spectra in dilute chloroform solution. The strong π–π stacking interactions evident in the X-ray crystal structures of these oligomers clearly influence their excited state electronic structures. However, while excimer formation[15] is the likely explanation of the solid state emission spectra additional studies are needed to confirm this.

In summary, two new conjugated oligoquinolines, **2a** and **2b**, have been synthesized and their molecular and photophysical properties were characterized. The obtained single crystal X-ray structures of these oligomers provide the first detailed structural information on the numerous polyquinolines.[3-9] Both **2a** and **2b** crystallized in a monoclinic lattice with different unit cell parameters and space groups. The X-ray crystal structures reveal that **2a** exhibits intermolecular face-to-face π-π stacking whereas **2b** manifests edge-to-face π-π stacking. The dilute solution and solid state optical absorption and emission spectra of **2b** were red-shifted from those of **2a** because of the greater degrees of π-electron delocalization and intramolecular charge transfer in **2b** compared to **2a**. The strongly Stokes shifted solid state emission bands of both oligomers are attributed to excimer formation. These conjugated oligoquinolines with known X-ray crystal structures are excellent model systems for elucidating the structures and properties of polyquinolines and may also find device applications as n-type semiconductors.

Acknowledgment. This research was supported by the Office of Naval Research and in part by the National Science Foundation (CTS-9311741).

Supporting Information Materials: Synthetic procedures and characterization of **2a** and **2b**, figures showing ^{1}H NMR spectra of **2a** and **2b**, experimental details for the X-ray crystallography and the tables of atomic coordinates, bond lengths, etc (21 pages). The material is contained in many libraries on microfiche, immediately follows this article in the microfilm version of the journal, can be ordered from the ACS, and can be

downloaded from the Internet; see any current masthead for ordering information and Internet access instructions.

References and Notes.

(1) See the comprehensive recent reviews on diverse p-type conjugated oligomers: (a) Müllen, K.; Wegner, G., Eds. *Electronic Materials: The Oligomer Approach*; Wiley-VCH: Weinheim, 1998. (b) Geerts, Y.; Klärner, G.; Müllen, K. *ibid*, pp. 1-103. (c) Baüerle, P., *ibid*, pp. 105-197. (d) Groenedaal, L.; Meijer, E. -W.; Vekemans, J. A. J. M., *ibid*, pp. 235-272.

(2) (a) Drefahl, G.; Plötner, G. *Chem. Ber.* **1961**, *94*, 907-914.(b) For a more recent study see Gill, R. E.; Meetsma, A.; Hadziioannou, G. *Adv. Mater.* **1996**, *8*, 212-214.

(3) (a) Sybert, P. D.; Beever, W. H.; Stille, J. K. *Macromolecules* **1981**, *14*, 493–502. (b) Pelter, M. W.; Stille, J. K. *Macromolecules* **1990**, *23*, 2418–2422.

(4) (a)Zimmerman, E. K.; Stille, J. K. *Macromolecules* **1985**, *18*, 321–327. (b) Abkowitz, M.A.; Stolka, M.; Antoniadis, H.; Agrawal, A. K.; Jenekhe, S. A. *Solid State Commun.* **1992**, *83*, 937-941.

(5) (a) Agrawal, A. K.; Jenekhe, S. A. *Chem. Mater.* **1992**, *4*, 95–104. (b) Agrawal, A. K.; Jenekhe, S. A. *Macromolecules* **1993**, *26*, 895–905. (c) Agrawal, A. K.; Jenekhe, S. A. *Chem. Mater.* **1996**, *8*, 579–589.

(6) Zhang, X.; Shetty, A. S. Jenekhe, S. A. *Acta Polymerica* **1998**, *49*, 52-55.

(7) (a) Jenekhe, S. A.; Zhang, X.; Chen, X. L.; Choong, V.-E.; Gao, Y.; Hsieh, B. R. *Chem. Mater.* **1997**, *9*, 409-412. (b) Zhang, X.; Shetty, A. S.; Jenekhe, S. A. *SPIE Proc.* **1997**, *3148*, 89-101.

(8) Agrawal, A. K.; Jenekhe, S. A.; Vanherzeele, H.; Meth, J. S. *J. Phys. Chem.* **1992**, *96*, 2837–2843.

(9) Sutherlin, D. M.; Stille, J. K. *Macromolecules* **1985**, *18*, 2669–2675.

(10) Friedlander, P. *Ber.* **1882**, *16*, 2572-2575.

(11) 2-Amino benzophenone, 1,4-diacetylbenzene, 4,4'-diacetylbiphenyl, and diphenylphosphate (Aldrich) were used without further purification. The synthetic procedure involved stirring a solution of 2-amino benzophenone (12.32 mmol), diketone (6.16 mmol), and diphenylphosphate (123 mmol) in freshly distilled m-cresol (3 mL) in a sealed tube at 140°C under an argon atmosphere. After six hours, the solution was cooled and poured into a solution of 10% triethylamine in methanol (300 mL) and the crude product was collected by filtration. The oligomers were purified by recrystallization from a 1:4 mixture of tetrahydrofuran and methanol.

2,2'-bis(4-phenylquinoline)-1,4-phenylene (2a). (3.23 g, 98 %). M.Pt. 251-252°C, Mass Spec. (EI) 484 (calc. for $C_{36}H_{24}N_2$), 484 (found), R_f (hexane:THF, 9:1) 0.4, ^{1}H NMR (300 MHz, $CDCl_3$): δ 8.52 (s, 4H), δ 8.31 (d, 2H), δ 7.97 (d, 2H), δ 7.94 (s, 2H), δ 7.78 (s, 2H), δ 7.6 (m, 12H). ^{13}C NMR (400 MHz, $CDCl_3$): δ 156.22, 149.3, 148.8, 104.3, 138.4, 130.2, 129.6, 128.6, 128.5, 128.1, 128.0, 126.5, 125.9, 125.7, 119.4, 119.3. **2,2'-bis(4-phenylquinoline)-4,4'-biphenylene (2b).** (1.5 g, 98 %) M.Pt. 252-253°C, Mass Spec. (EI) 560 (calc. for $C_{42}H_{28}N_2$), 560 (found), R_f (hexane:THF, 6:1) 0.49, ^{1}H NMR (300 MHz, $CDCl_3$): δ 8.36 (d, 4H), δ 8.31 (d, 2H), δ 7.95 (d, 2H), δ 7.90 (s, 2H), δ 7.85 (d, 4H), δ 7.78 (t, 2H), δ 7.55 (m, 12H) δ 7.50 (t, 2H). ^{13}C NMR (400MHz, $CDCl_3$): 156.3, 149.2, 148.9, 141.4, 138.8, 138.4, 130.2, 129.6, 128.6, 128.4, 128.0, 127.5, 126.4, 125.8, 125.7, 119.3, 119.2.

(12) (a) Williams, J. H. *Acc. Chem. Res.* **1993**, *26*, 593-598. (b) Desiraju, G. R.; Gavezzotti, A. *J. Chem. Soc., Chem. Commun.* **1989**, 621-623.

(13) (a) Guilbault, G. G., Ed. *Practical Fluorescence*; Marcel Dekker Inc: New York, 1990, Chapter 1. (b) Wehry, E. L. *ibid*, Chapter 4 and references therein. (c) Demas, J. N.; Crosby, G. A. *J. Phys. Chem.* **1971**, *75*, 991-1024. (d) Osaheni, J. A.; Jenekhe, S. A. *J. Am. Chem. Soc.* **1995**, *117*, 7389-7398.

(14) Slama-Schwok, A.; Blanchard-Desce, M.; Lehn, J. -M. *J. Phys. Chem.* **1990**, *94*, 3894-3902.

(15) Jenekhe, S. A.; Osaheni, J. A. *Science* **1994**, *265*, 765-768.

Figure Captions

Figure 1. (A) 30% ORTEP diagram of oligomer **2a** with atom numbering scheme. Because the molecule has an inversion center at the midpoint of the central phenylene ring, the symmetry related atoms are not labeled. (B) The organization of the molecules in a single unit cell and (C) the packing of the molecule along the b-axis is shown with intermolecular distance of 4 Å.

Figure 2. (A) 30% ORTEP diagram of oligomer **2b** with atom numbering scheme. Because the molecule has an inversion center at the midpoint of the central C-C bond, the symmetry related atoms are not labeled. (B) The organization of the molecules in a single unit cell and (C) the packing of the molecule with intermolecular distance of 3.6 Å. Note the edge-to-face π-stacking between the pendant phenyl groups and the biphenylene moieties in C.

Figure 3. Optical absorption and fluorescence spectra of oligomers **2a** (dashed lines) and **2b** (solid lines) in (A) chloroform (2×10^{-5} M) and (B) formic acid (2×10^{-5} M).

Figure 4. Absorption and emission spectra of spin coated thin films of oligomers **2a** (dashed lines) and **2b** (solid lines) on fused silica substrates after annealing at 70°C.

Scheme 1

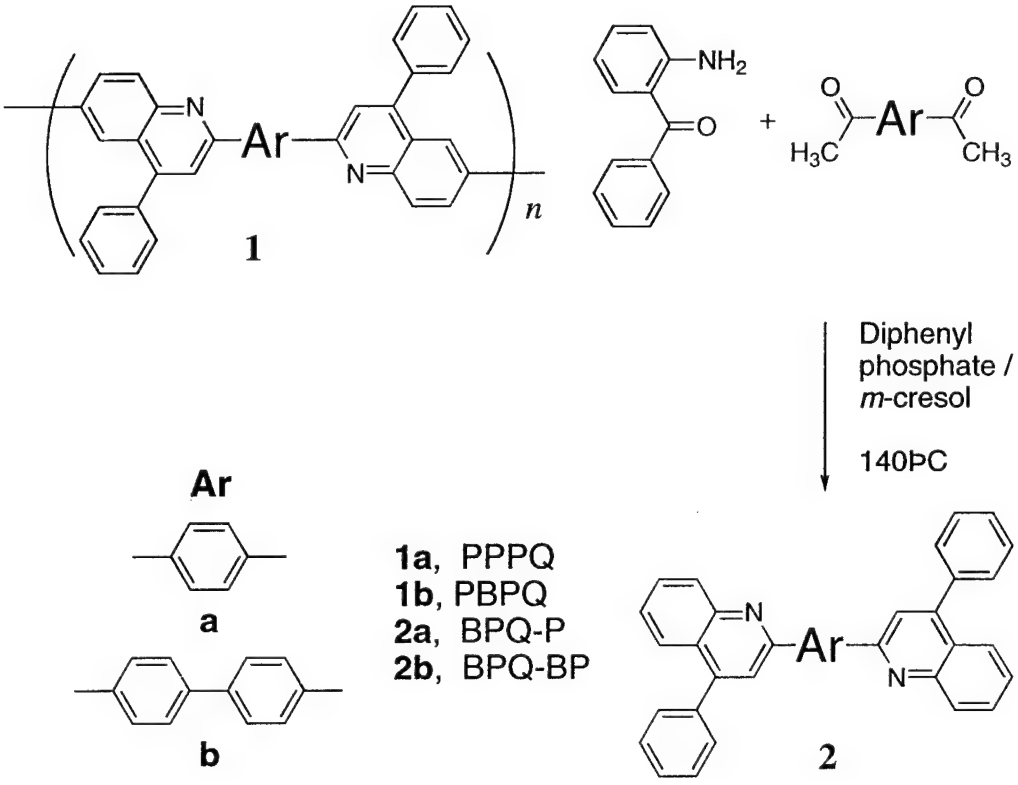
N
Ar
N
n
1
NH2
O
+
O
Ar
O
H3C
CH3
Diphenyl
phosphate /
m-cresol
140ºC
Ar
a
b
1a, PPPQ
1b, PBPQ
2a, BPQ-P
2b, BPQ-BP
N
Ar
N
2

Figure 1.

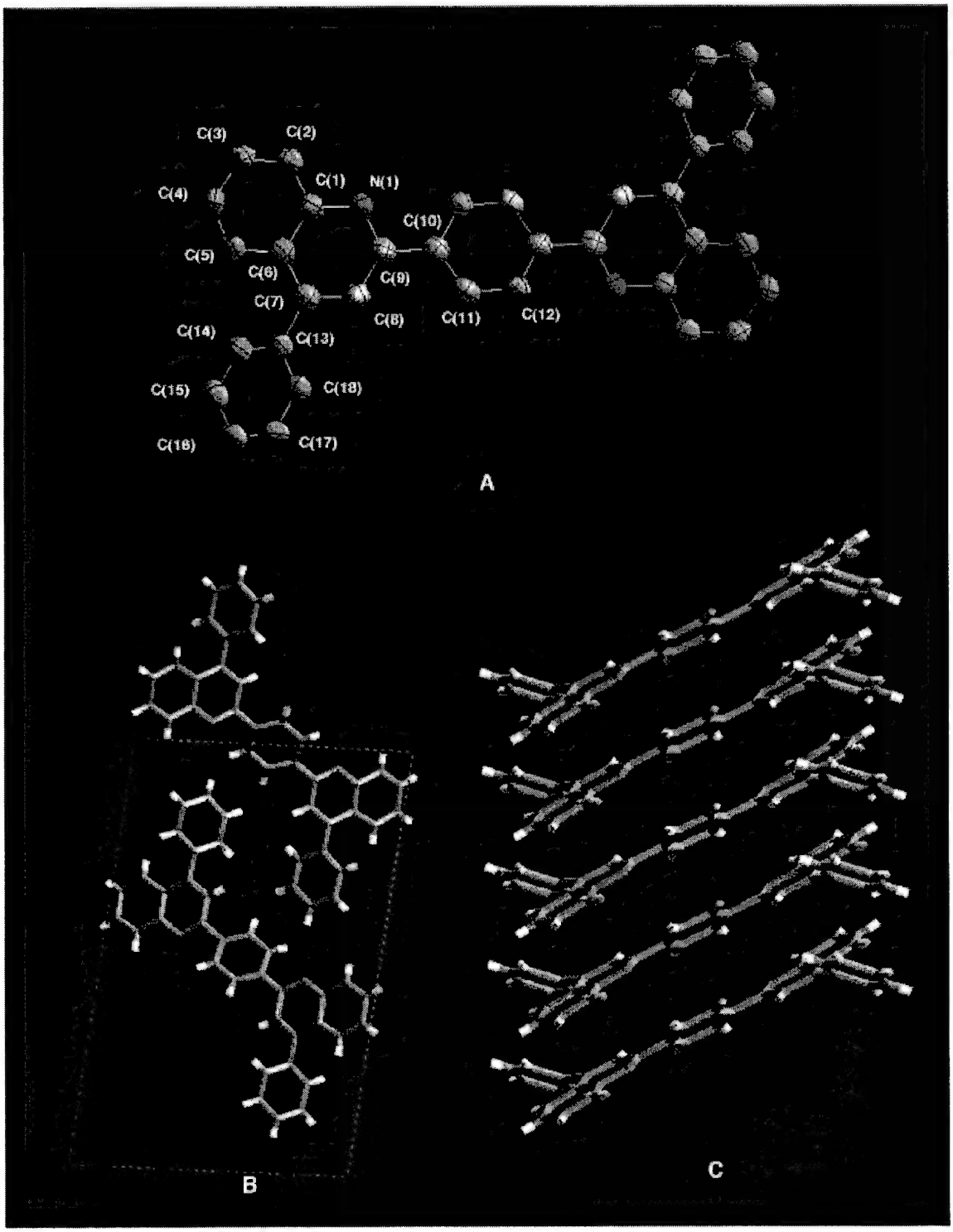
C(3)
C(2)
C(1)
N(1)
C(4)
C(10)
C(5)
C(6)
C(9)
C(7)
C(8)
C(11)
C(12)
C(14)
C(13)
C(15)
C(18)
C(16)
C(17)
A
B
C

Figure 2.

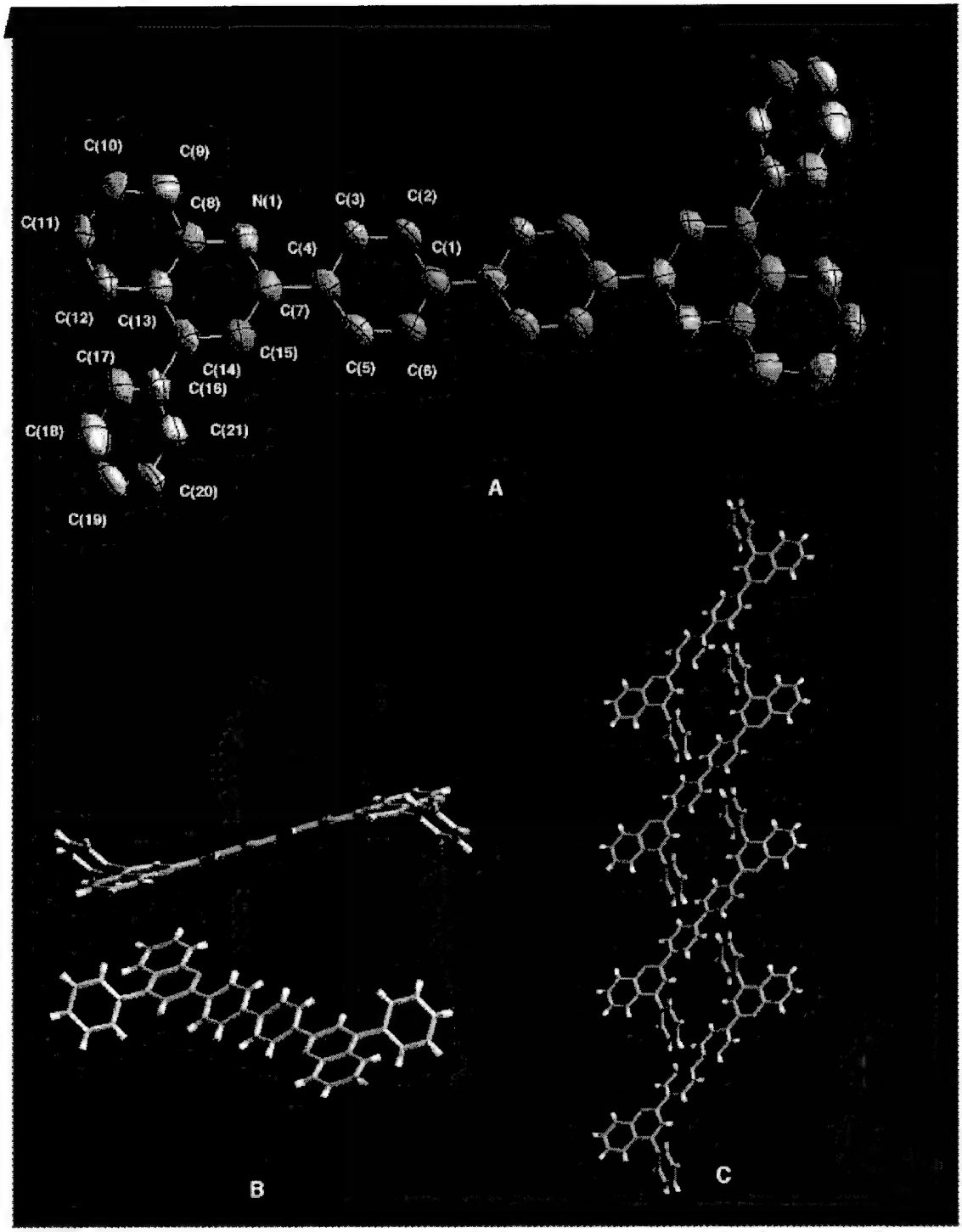
C(10)
C(9)
C(8)
N(1)
C(3)
C(2)
C(11)
C(4)
C(1)
C(12)
C(13)
C(7)
C(15)
C(17)
C(14)
C(5)
C(6)
C(16)
C(18)
C(21)
C(20)
C(19)
A
B
C

Figure 3.

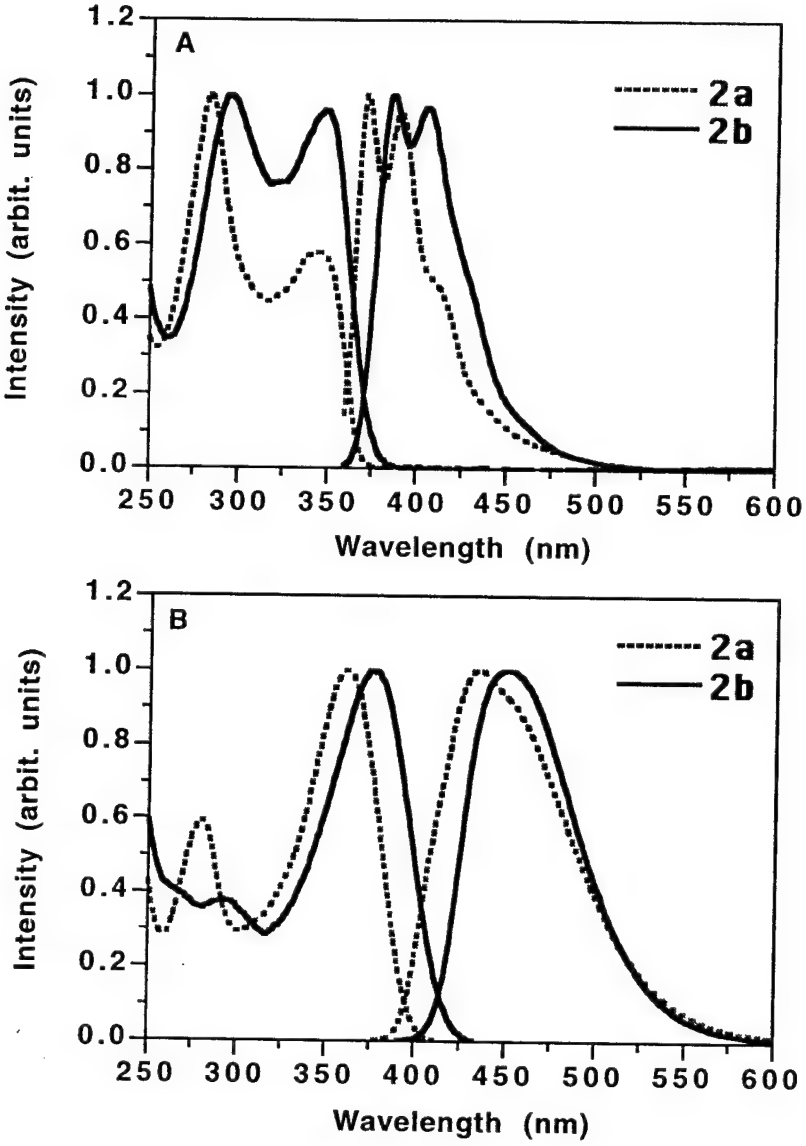
A
2a
2b
Intensity (arbit. units)
Wavelength (nm)
B
2a
2b
Intensity (arbit. units)
Wavelength (nm)

Figure 4.

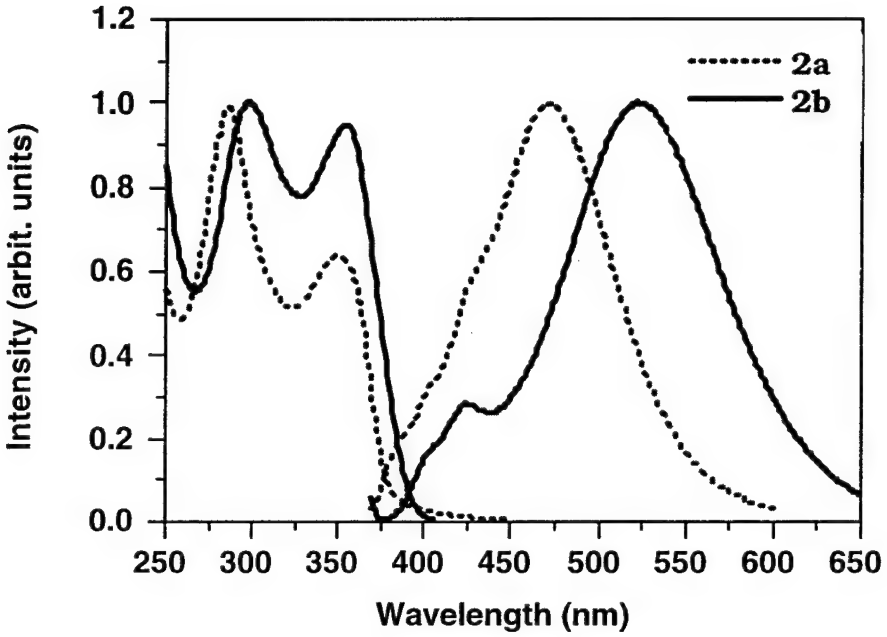
1.2
1.0
0.8
0.6
0.4
0.2
0.0
Intensity (arbit. units)
250
300
350
400
450
500
550
600
650
Wavelength (nm)
2a
2b

[1]SUPPLEMENTARY MATERIAL

to:

X-ray Crystal Structures and Photophysical Properties of New Conjugated Oligoquinolines.

Ashok S. Shetty,[†] Elizabeth B. Liu,[†] Rene J. Lachicotte,[§] and Samson A. Jenekhe*[,†,§]

Departments of Chemical Engineering and Chemistry and Center for Photoinduced Charge Transfer, University of Rochester, Rochester, New York 14627-0166.

Synthetic procedure, ^{1}H NMR, ^{13}C NMR, mass spectroscopic, R_f and melting point data of oligomers, 2,2'-bis(4-phenylquinoline)-1,4-phenylene (**2a**). page 2

Synthetic procedure, ^{1}H NMR, ^{13}C NMR, mass spectroscopic, R_f and melting point data of oligomers, 2,2'-bis(4-phenylquinoline)-4,4'-biphenylene (**2b**). page 2

Figure S1. ^{1}H NMR of Oligomer **2a** in deuterated chloroform at room temperature. page 3

Figure S2. ^{1}H NMR of Oligomer **2b** in deuterated chloroform at room temperature. page 4

Experimental details for the X-ray Crystallography. page 5

Tables of Atomic coordinates, Bond lengths, Anisotropic Displacement Parameters, and Hydrogen Coordinates for **2a** and **2b** page 7-21

[†] Department of Chemical Engineering and Center for Photoinduced Charge Transfer.
[§] Department of Chemistry.

Preparation of 2,2'-bis(4-phenylquinoline)-1,4-phenylene (2a). A mixture of 2-aminobenzophenone (3g, 18.5 mmol), 1,4-diacetylbenzene (1.0 g, 6.16 mmol) and diphenylphosphate (10g, 40 mmol) in m-cresol (30 mL) was refluxed at 150°C under nitrogen atmosphere for 8h. After cooling to R.T., the product was precipitated out by pouring the reaction mixture into methanol (500 mL). The crude product was recrystallized from a methanol:ethylacetate (9:1) mixture to yield colorless needles (2.93 g, 98% yield). M.Pt. 251-252°C, Mass Spec. (EI) 484 (calc. for $C_{36}H_{24}N_2$), 484 (found), R_f (hexane:THF, 9:1) 0.4, ^{1}H NMR (300 MHz, $CDCl_3$): δ 8.52 (s, 4H), δ 8.31 (d, 2H), δ 7.97 (d, 2H), δ 7.94 (s, 2H), δ 7.78 (s, 2H), δ 7.6 (m, 12H). ^{13}C NMR (400 MHz, $CDCl_3$): δ 156.22, 149.3, 148.8, 104.3, 138.4, 130.2, 129.6, 128.6, 128.5, 128.1, 128.0, 126.5, 125.9, 125.7, 119.4, 119.3.

Preparation of 2,2'-bis(4-phenylquinoline)-4,4'-biphenylene (2b). A mixture of 2-aminobenzophenone (1.24 g, 6.28 mmol), 1,4-diacetylbiphenyl (0.5 g, 2.1 mmol) and diphenylphosphate (1 g, 4 mmol) in m-cresol (1.8 mL) was refluxed at 150°C under nitrogen atmosphere for 8h. After cooling to R.T., the product was precipitated out by pouring the reaction mixture into methanol (500 mL). The crude product was recrystallized from a methanol:ethylacetate (9:1) mixture to yield colorless needles (1.1 g, 94 % yield). M.Pt. 252-253°C, Mass Spec. (EI) 560 (calc. for $C_{42}H_{28}N_2$), 560 (found), R_f (hexane:THF, 6:1) 0.49, ^{1}H NMR (300 MHz, $CDCl_3$): δ 8.36 (d, 4H), δ 8.31 (d, 2H), δ 7.95 (d, 2H), δ 7.90 (s, 2H), δ 7.85 (d, 4H), δ 7.78 (t, 2H), δ 7.55 (m, 12H) δ 7.50 (t, 2H). ^{13}C NMR (400MHz, $CDCl_3$): 156.3, 149.2, 148.9, 141.4, 138.8, 138.4, 130.2, 129.6, 128.6, 128.4, 128.0, 127.5, 126.4, 125.8, 125.7, 119.3, 119.2

Figure S1

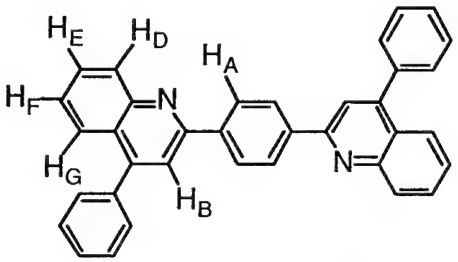

2a

^{1}H NMR in $CDCl_3$

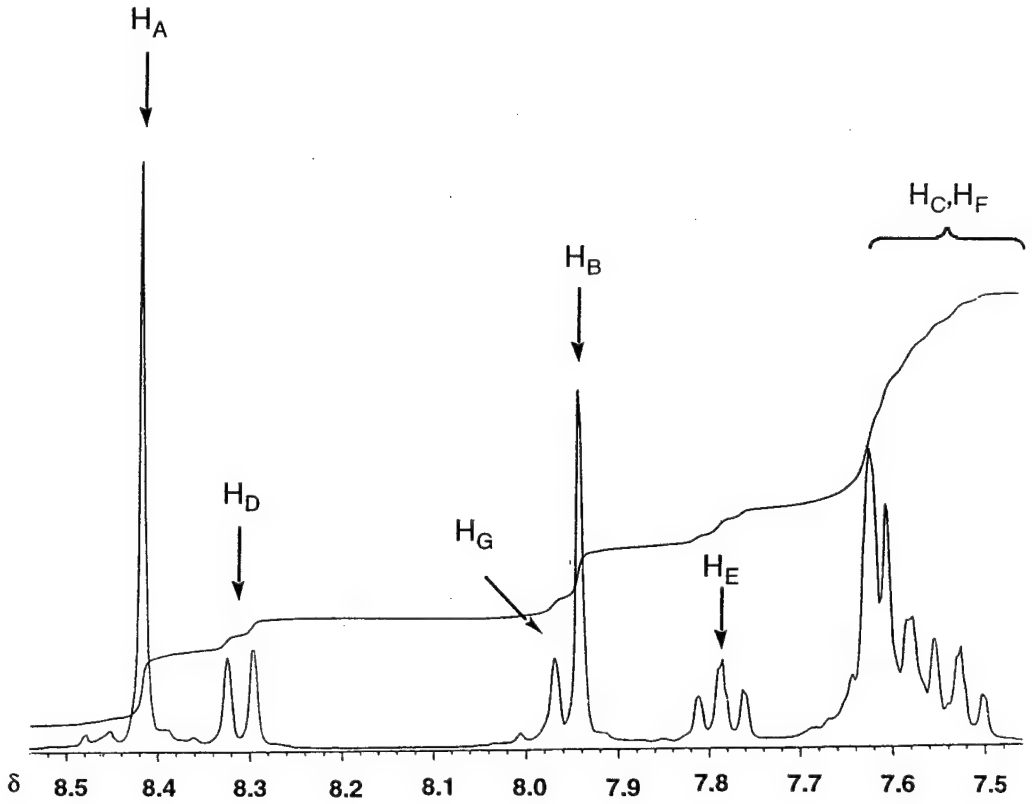

Figure S2

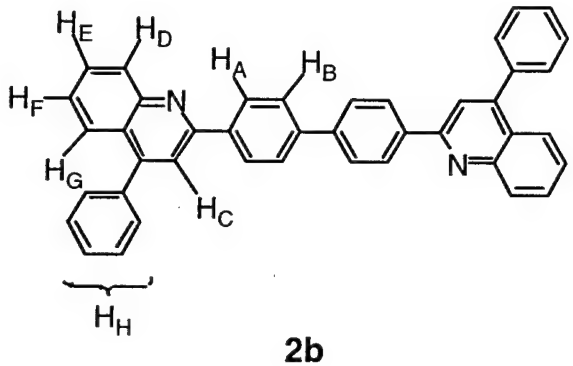

2b

^{1}H NMR in $CDCl_3$

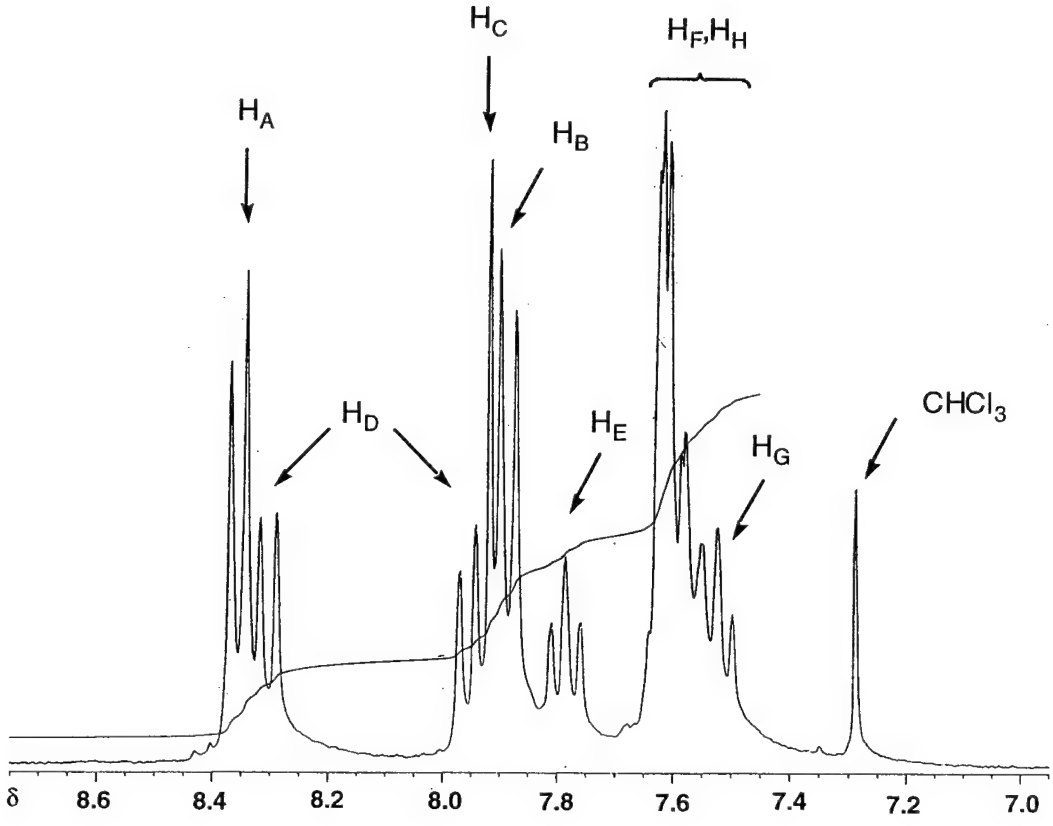

Experimental Details of the X-ray Crystallography.

Crystals of **2a** and **2b** were each cut and mounted under Paratone-8277 on glass fibers, and immediately placed on the X-ray diffractometer in a cold nitrogen stream supplied by a Siemens LT-2A low temperature device. The X-ray intensity data were collected on a standard Siemens SMART CCD Area Detector System equipped with a normal focus molybdenum-target X-ray tube operated at 2.0 kW (50 kV, 40 mA). A total of 1321 frames of data (1.3 hemispheres) were collected using a narrow frame method with scan widths of 0.3° in ω, and exposure times of 30 sec/frame using a crystal-to-detector distance of 5.094 cm. (maximum 2θ angle of 56.52°). The total data collection time was approximately 12 hours for each crystal. Frames were integrated with the Siemens SAINT program to yield: for **2a**,[1] a total of 4342 reflections, of which 1543 were independent (R_{int} = 2.82 %, R_{sig} = 2.72 %)[2] and 1404 were above $2\sigma(I)$; for **2b**, a total of 8282 reflections, of which 3333 were independent (R_{int} = 1.90 %, R_{sig} = 2.64 %) and 2605 were above $2\sigma(I)$. The unit cell parameters, provided in Table 1, were based upon the least-squares refinement of three dimensional centroids of 3162 reflections for **2a** and 4688 reflections for **2b**. The space group assignments were made on the basis of systematic absences and intensity statistics by using the XPREP program (Siemens, SHELXTL 5.04). The structures were solved by using direct methods and refined by full-matrix least-squares on F^2. All non-hydrogen atoms were refined with anisotropic thermal parameters, and all of the hydrogens were included in idealized positions. The structures refined to: for **2a**, a goodness of fit (GOF)[3] of 1.198 and final residuals[4] ($I > 2\sigma(I)$) of R_1 = 3.95 %, and wR_2 = 8.88 %; for **2b**, a goodness of fit (GOF) of 1.085 and final residuals ($I > 2\sigma(I)$) of R_1 = 4.52 %, and wR_2 = 11.50 %.

[1] $R_{int} = \sum | F_0^2 - F_0^2(\text{mean}) | / \sum [F_0^2]$; $R_{sigma} = \sum [\sigma(F_0^2)] / \sum [F_0^2]$

[2] Although data were collected to a maximum 2θ angle of 56.50° for **2a**, there were essentially no observed data > 45° and therefore these data were omitted.

[3] $GOF = [\sum[w(F_0^2 - F_c^2)^2]/(n-p)]^{1/2}$, where n and p denote the number of data and parameters

[4] $R_1 = (\Sigma \| F_o | - | F_c \|) / \Sigma | F_o |$, $wR_2 = [\Sigma[w(F_o^2-F_c^2)^2] / \Sigma[w(F_o^2)^2]]^{1/2}$, where $w = 1/[\sigma^2(F_o^2) + (a\cdot P)^2 + b\cdot P]$ and $P = [f\cdot(\text{Maximum of 0 or } F_o^2) + (1-f)\cdot F_c^2]$

Table 1. Crystal and Structure Refinement Data for **2a** and **2b**

Crystal Parameters	**2a**	**2b**
chemical formula	$C_{36}H_{24}N_2$	$C_{42}H_{28}N_2$
formula weight	484.57	562.68
crystal system	Monoclinic	Monoclinic
space group (No.)	$P2/c$ (#13)	$P2_1/c$ (#14)
Z	2	2
a, Å[a]	13.9932(8)	11.4460(2)
b, Å	4.0104(2)	8.3789(2)
c, Å	21.6130(13)	15.8601(3)
β, deg	96.0320(10)	105.9710(10)
Volume, Å^3	1206.17(12)	1462.35(5)
ρ_{calc}, Kg/m^3	1.334	1.278
crystal dimens, mm	0.05 x 0.06 x 0.18	0.30 x 0.34 x 0.38
temperature, °C	-100	-80
Measurement of Intensity Data and Structure Refinement		
diffractometer	Siemens SMART	Siemens SMART
radiation, λ, Å	Mo, 0.71073	Mo, 0.71073
2θ range for data collection (deg)[b]	3 - 56	4 - 56
limiting indices	$-18 \le h \le 18$	$-15 \le h \le 14$
	$-5 \le k \le 5$	$-10 \le k \le 6$
	$-14 \le l \le 28$	$-20 \le l \le 19$
total reflections	4342(to 45°)[c]	8282
independent reflections	1543 [R(int) = 0.0282]	3333 [R(int) = 0.0190]
no. of observed data	1404 ($I > 2\sigma(I)$)	2605 ($I > 2\sigma(I)$)
no. of parameters varied	173	200

μ, mm^{-1}	0.078	0.074
absorption correction	NA	Empirical (SADABS)
range of trans. factors		0.850 - 0.714
$R_1(F_o)$, $wR_2(F_o^2)$ %, $(I>2\sigma(I))^d$	3.95, 8.88	4.52, 11.50
$R_1(F_o)$, $wR_2(F_o^2)$ %, all data	4.59, 9.28	6.11, 12.33
goodness-of-fit on F^2	1.198	1.085

[a] It has been noted that the integration program SAINT produces cell constant errors that are unreasonably small, since systematic error is not included. More reasonable errors might be estimated at 10x the listed values. [b] The SMART CCD crystal-to-detector distance is set to 5.094 cm which equates to a maximum 2θ angle of 56.52°. [c]Although data are routinely collected to 56°, these crystals were weak diffracters and therefore data greater than 45° were omitted from the refinement. [d] $R_1 = (\Sigma \| F_o | - | F_c \|) / \Sigma | F_o |$, $wR_2 = [\Sigma[w(F_o^2-F_c^2)^2] / \Sigma[w(F_o^2)^2]]^{1/2}$, where $w = 1/[\sigma^2(F_o^2) + (a\cdot P)^2 + b\cdot P]$ and $P = [f\cdot(\text{Maximum of 0 or } F_o^2) + (1-f)\cdot F_c^2]$

Table 1. Crystal data and structure refinement for **2a**

Identification code	jenas2t
Empirical formula	C36 H24 N2
Formula weight	484.57
Temperature	173(2) K
Wavelength	0.71073 Å
Crystal system	Monoclinic
Space group	P2/c
Unit cell dimensions	a = 13.9932(8) A alpha = 90 deg. b = 4.0104(2) A beta = 96.0320(10) deg. c = 21.6130(13) A gamma = 90 deg.
Volume, Z	1206.17(12) A^3, 2
Density (calculated)	1.334 Kg/m^3
Absorption coefficient	0.078 mm^-1
F(000)	508
Crystal size	0.05 x 0.06 x 0.18 mm
Theta range for data collection	1.46 to 22.49 deg.
Limiting indices	$-18 \le h \le 18$, $-5 \le k \le 5$, $-14 \le l \le 28$
Theta range for data refinement	1.46 to 22.49 deg.
Reflections collected	4342
Independent reflections	1543 [R(int) = 0.0282]
Absorption correction	None
Refinement method	Full-matrix least-squares on F^2
Data / restraints / parameters	1543 / 0 / 173
Goodness-of-fit on F^2	1.198
Final R indices [I>2sigma(I)]	R1 = 0.0395, wR2 = 0.0888
R indices (all data)	R1 = 0.0459, wR2 = 0.0928
Extinction coefficient	0.013(2)
Largest diff. peak and hole	0.135 and -0.147 e.A^-3

Table 2. Atomic coordinates (x 10^4) and equivalent isotropic displacement parameters (A^2 x 10^3) for **2a**. U(eq) is defined as one third of the trace of the orthogonalized Uij tensor.

	x	y	z	U(eq)
N(1)	7367(1)	3722(4)	5464(1)	26(1)
C(1)	8130(1)	5226(4)	5804(1)	24(1)
C(2)	8909(1)	6218(5)	5483(1)	29(1)
C(3)	9685(1)	7791(5)	5784(1)	32(1)
C(4)	9715(1)	8458(5)	6424(1)	31(1)
C(5)	8974(1)	7543(5)	6746(1)	28(1)
C(6)	8158(1)	5877(4)	6452(1)	24(1)
C(7)	7346(1)	4881(4)	6755(1)	23(1)
C(8)	6588(1)	3476(4)	6398(1)	25(1)
C(9)	6613(1)	2923(4)	5753(1)	24(1)
C(10)	5786(1)	1389(4)	5373(1)	23(1)
C(11)	4850(1)	1735(4)	5530(1)	25(1)
C(12)	4078(1)	374(5)	5165(1)	25(1)
C(13)	7299(1)	5281(5)	7437(1)	25(1)
C(14)	8034(1)	4150(5)	7869(1)	29(1)
C(15)	7957(1)	4378(5)	8499(1)	33(1)
C(16)	7154(1)	5784(5)	8713(1)	34(1)
C(17)	6421(1)	6938(5)	8290(1)	34(1)
C(18)	6490(1)	6671(5)	7658(1)	30(1)

Table 3. Bond lengths [A] and angles [deg] for **2a**.

N(1)-C(9)	1.321(2)
N(1)-C(1)	1.370(2)
C(1)-C(2)	1.409(2)
C(1)-C(6)	1.422(2)
C(2)-C(3)	1.361(3)
C(3)-C(4)	1.404(3)
C(4)-C(5)	1.359(2)
C(5)-C(6)	1.415(2)
C(6)-C(7)	1.427(2)
C(7)-C(8)	1.366(2)
C(7)-C(13)	1.491(2)
C(8)-C(9)	1.415(2)
C(9)-C(10)	1.481(2)
C(10)-C(12)#1	1.391(2)
C(10)-C(11)	1.393(2)
C(11)-C(12)	1.381(2)
C(12)-C(10)#1	1.391(2)
C(13)-C(14)	1.390(2)
C(13)-C(18)	1.391(2)
C(14)-C(15)	1.381(3)
C(15)-C(16)	1.378(3)
C(16)-C(17)	1.381(3)
C(17)-C(18)	1.383(2)
C(9)-N(1)-C(1)	118.0(2)
N(1)-C(1)-C(2)	117.4(2)
N(1)-C(1)-C(6)	123.2(2)
C(2)-C(1)-C(6)	119.4(2)
C(3)-C(2)-C(1)	121.0(2)
C(2)-C(3)-C(4)	119.9(2)
C(5)-C(4)-C(3)	120.5(2)
C(4)-C(5)-C(6)	121.4(2)
C(5)-C(6)-C(1)	117.8(2)
C(5)-C(6)-C(7)	124.7(2)
C(1)-C(6)-C(7)	117.4(2)
C(8)-C(7)-C(6)	117.7(2)
C(8)-C(7)-C(13)	119.4(2)
C(6)-C(7)-C(13)	122.9(2)
C(7)-C(8)-C(9)	121.5(2)
N(1)-C(9)-C(8)	122.1(2)
N(1)-C(9)-C(10)	117.0(2)
C(8)-C(9)-C(10)	120.8(2)
C(12)#1-C(10)-C(11)	117.9(2)

C(12)#1-C(10)-C(9)	120.5(2)
C(11)-C(10)-C(9)	121.6(2)
C(12)-C(11)-C(10)	121.4(2)
C(11)-C(12)-C(10)#1	120.7(2)
C(14)-C(13)-C(18)	118.1(2)
C(14)-C(13)-C(7)	121.6(2)
C(18)-C(13)-C(7)	120.3(2)
C(15)-C(14)-C(13)	120.8(2)
C(16)-C(15)-C(14)	120.5(2)
C(15)-C(16)-C(17)	119.4(2)
C(16)-C(17)-C(18)	120.2(2)
C(17)-C(18)-C(13)	121.0(2)

Symmetry transformations used to generate equivalent atoms:
#1 -x+1,-y,-z+1

Table 4. Anisotropic displacement parameters (A^2 x 10^3) for **2a**.
The anisotropic displacement factor exponent takes the form:
-2 pi^2 [h^2 a*^2 U11 + ... + 2 h k a* b* U12]

	U11	U22	U33	U23	U13	U12
N(1)	25(1)	29(1)	22(1)	1(1)	2(1)	2(1)
C(1)	24(1)	24(1)	23(1)	1(1)	1(1)	4(1)
C(2)	29(1)	36(1)	23(1)	1(1)	4(1)	2(1)
C(3)	26(1)	37(1)	34(1)	4(1)	9(1)	0(1)
C(4)	26(1)	34(1)	33(1)	-2(1)	1(1)	-4(1)
C(5)	27(1)	30(1)	27(1)	-4(1)	1(1)	1(1)
C(6)	25(1)	21(1)	24(1)	1(1)	0(1)	6(1)
C(7)	26(1)	20(1)	24(1)	1(1)	2(1)	4(1)
C(8)	26(1)	27(1)	24(1)	3(1)	5(1)	1(1)
C(9)	28(1)	22(1)	21(1)	3(1)	2(1)	5(1)
C(10)	27(1)	23(1)	20(1)	5(1)	1(1)	1(1)
C(11)	33(1)	24(1)	18(1)	0(1)	3(1)	1(1)
C(12)	25(1)	28(1)	23(1)	2(1)	4(1)	2(1)
C(13)	28(1)	25(1)	21(1)	-1(1)	2(1)	-3(1)
C(14)	31(1)	31(1)	26(1)	-3(1)	3(1)	1(1)
C(15)	40(1)	36(1)	23(1)	0(1)	-1(1)	-3(1)
C(16)	44(1)	36(1)	23(1)	-3(1)	7(1)	-7(1)
C(17)	37(1)	36(1)	29(1)	-3(1)	12(1)	-1(1)
C(18)	29(1)	33(1)	28(1)	0(1)	3(1)	0(1)

Table 5. Hydrogen coordinates (x 10^4) and isotropic displacement parameters (A^2 x 10^3) for **2a**.

	x	y	z	U(eq)
H(2A)	8892(1)	5783(5)	5050(1)	35
H(3A)	10206(1)	8435(5)	5562(1)	38
H(4A)	10257(1)	9559(5)	6633(1)	37
H(5A)	9004(1)	8032(5)	7178(1)	34
H(8A)	6031(1)	2856(4)	6587(1)	30
H(11A)	4740(1)	2933(4)	5895(1)	30
H(12A)	3448(1)	644(5)	5283(1)	30
H(14A)	8596(1)	3207(5)	7729(1)	35
H(15A)	8461(1)	3560(5)	8788(1)	40
H(16A)	7107(1)	5957(5)	9147(1)	41
H(17A)	5867(1)	7918(5)	8433(1)	40
H(18A)	5978(1)	7449(5)	7371(1)	36

Table 1. Crystal data and structure refinement for **2b**.

Identification code	sad/jenas10
Empirical formula	C42 H28 N2
Formula weight	562.68
Temperature	193(2) K
Wavelength	0.71073 Å
Crystal system	Monoclinic
Space group	P2(1)/c
Unit cell dimensions	a = 11.4460(2) Å alpha = 90 deg.
	b = 8.3789(2) Å beta = 105.9710(10) deg.
	c = 15.8601(3) Å gamma = 90 deg.
Volume, Z	1462.35(5) A^3, 2
Density (calculated)	1.278 Kg/m^3
Absorption coefficient	0.074 mm^-1
F(000)	592
Crystal size	0.30 x 0.34 x 0.38 mm
Theta range for data collection	1.85 to 28.27 deg.
Limiting indices	$-15 \le h \le 14$, $-10 \le k \le 6$, $-20 \le l \le 19$
Reflections collected	8282
Independent reflections	3333 [R(int) = 0.0190]
Reflections >2sigI	2605
Absorption correction	SADABS
Max & Min Transmission	0.850 0.714
Refinement method	Full-matrix least-squares on F^2
Data / restraints / parameters	3333 / 0 / 200
Goodness-of-fit on F^2	1.085
Final R indices [I>2sigma(I)]	R1 = 0.0452, wR2 = 0.1150
R indices (all data)	R1 = 0.0611, wR2 = 0.1233
Extinction coefficient	0.019(3)
Largest diff. peak and hole	0.217 and -0.167 e.A^-3

Table 6. Atomic coordinates (x 10^4) and equivalent isotropic displacement parameters (A^2 x 10^3) for **2b**. U(eq) is defined as one third of the trace of the orthogonalized Uij tensor.

	x	y	z	U(eq)
N(1)	3656(1)	5023(1)	735(1)	40(1)
C(1)	546(1)	9484(2)	154(1)	36(1)
C(2)	591(1)	7957(2)	-166(1)	61(1)
C(3)	1609(1)	7005(2)	116(1)	58(1)
C(4)	2638(1)	7535(2)	730(1)	36(1)
C(5)	2586(1)	9042(2)	1071(1)	54(1)
C(6)	1563(1)	9991(2)	789(1)	54(1)
C(7)	3757(1)	6537(2)	983(1)	36(1)
C(8)	4689(1)	4105(2)	940(1)	39(1)
C(9)	4569(1)	2474(2)	706(1)	47(1)
C(10)	5559(1)	1492(2)	910(1)	53(1)
C(11)	6708(1)	2078(2)	1354(1)	54(1)
C(12)	6858(1)	3647(2)	1575(1)	48(1)
C(13)	5858(1)	4717(2)	1368(1)	38(1)
C(14)	5947(1)	6374(2)	1580(1)	37(1)
C(15)	4889(1)	235(2)	1418(1)	38(1)
C(16)	7130(1)	7211(2)	1917(1)	38(1)
C(17)	8029(1)	7073(2)	1477(1)	46(1)
C(18)	9101(1)	7933(2)	1763(1)	57(1)
C(19)	9286(1)	8937(2)	2479(1)	59(1)
C(20)	8397(1)	092(2)	2910(1)	53(1)
C(21)	7329(1)	8235(2)	2631(1)	44(1)

Table 7. Bond lengths [A] and angles [deg] for **2b**.

N(1)-C(7)	1.324(2)
N(1)-C(8)	1.372(2)
C(1)-C(6)	1.379(2)
C(1)-C(2)	1.384(2)
C(1)-C(1)#1	1.488(2)
C(2)-C(3)	1.381(2)
C(3)-C(4)	1.379(2)
C(4)-C(5)	1.381(2)
C(4)-C(7)	1.490(2)
C(5)-C(6)	1.384(2)
C(7)-C(15)	1.416(2)
C(8)-C(9)	1.413(2)
C(8)-C(13)	1.420(2)
C(9)-C(10)	1.366(2)
C(10)-C(11)	1.399(2)
C(11)-C(12)	1.360(2)
C(12)-C(13)	1.419(2)
C(13)-C(14)	1.426(2)
C(14)-C(15)	1.371(2)
C(14)-C(16)	1.487(2)
C(16)-C(21)	1.390(2)
C(16)-C(17)	1.397(2)
C(17)-C(18)	1.387(2)
C(18)-C(19)	1.381(2)
C(19)-C(20)	1.379(2)
C(20)-C(21)	1.381(2)
C(7)-N(1)-C(8)	117.82(11)
C(6)-C(1)-C(2)	116.38(12)
C(6)-C(1)-C(1)#1	121.7(2)

C(2)-C(1)-C(1)#1	121.93(14)
C(3)-C(2)-C(1)	121.87(13)
C(4)-C(3)-C(2)	121.56(14)
C(3)-C(4)-C(5)	116.78(12)
C(3)-C(4)-C(7)	120.89(12)
C(5)-C(4)-C(7)	122.30(11)
C(4)-C(5)-C(6)	21.52(13)
C(1)-C(6)-C(5)	121.83(13)
N(1)-C(7)-C(15)	122.29(11)
N(1)-C(7)-C(4)	117.34(11)
C(15)-C(7)-C(4)	120.21(12)
N(1)-C(8)-C(9)	117.66(12)
N(1)-C(8)-C(13)	123.30(12)
C(9)-C(8)-C(13)	119.04(12)
C(10)-C(9)-C(8)	120.40(14)
C(9)-C(10)-C(11)	120.82(14)
C(12)-C(11)-C(10)	120.22(14)
C(11)-C(12)-C(13)	121.00(14)
C(12)-C(13)-C(8)	118.49(13)
C(12)-C(13)-C(14)	124.07(12)
C(8)-C(13)-C(14)	117.43(11)
C(15)-C(14)-C(13)	117.77(12)
C(15)-C(14)-C(16)	119.30(12)
C(13)-C(14)-C(16)	122.83(11)
C(14)-C(15)-C(7)	121.12(12)
C(21)-C(16)-C(17)	118.69(13)
C(21)-C(16)-C(14)	120.79(12)
C(17)-C(16)-C(14)	120.34(12)
C(18)-C(17)-C(16)	120.05(14)
C(19)-C(18)-C(17)	120.4(2)
C(20)-C(19)-C(18)	119.8(2)

C(19)-C(20)-C(21)	120.1(2)
C(20)-C(21)-C(16)	120.88(14)

Symmetry transformations used to generate equivalent atoms:

#1 -x,-y+2,-z

Table 8. Anisotropic displacement parameters (A^2 x 10^3) for **2b**.

The anisotropic displacement factor exponent takes the form:

-2 pi^2 [h^2 a*^2 U11 + ... + 2 h k a* b* U12]

	U11	U22	U33	U23	U13	U12
N(1)	38(1)	39(1)	43(1)	2(1)	12(1)	1(1)
C(1)	29(1)	43(1)	38(1)	-4(1)	1`(1)	1(1)
C(2)	38(1)	62(1)	69(1)	-31(1)	-9(1)	11(1)
C(3)	42(1)	52(1)	72(1)	-26(1)	-1(1)	9(1)
C(4)	31(1)	40(1)	39(1)	1(1)	11(1)	2(1)
C(5)	36(1)	49(1)	64(1)	-14(1)	-6(1)	4(1)
C(6)	38(1)	42(1)	72(1)	-18(1)	-3(1)	5(1)
C(7)	33(1)	39(1)	38(1)	3(1)	12(1)	2(1)
C(8)	42(1)	38(1)	39(1)	6(1)	13(1)	4(1)
C(9)	52(1)	41(1)	47(1)	2(1)	12(1)	1(1)
C(10)	68(1)	36(1)	57(1)	7(1)	18(1)	7(1)
C(11)	56(1)	41(1)	62(1)	14(1)	14(1)	16(1)
C(12)	43(1)	46(1)	54(1)	12(1)	11(1)	1`(1)
C(13)	40(1)	38(1)	38(1)	9(1)	12(1)	5(1)
C(14)	35(1)	40(1)	36(1)	7(1)	1`(1)	4(1)
C(15)	35(1)	38(1)	42(1)	2(1)	10(1)	3(1)
C(16)	32(1)	38(1)	43(1)	9(1)	7(1)	6(1)
C(17)	41(1)	48(1)	52(1)	6(1)	15(1)	5(1)
C(18)	38(1)	58(1)	77(1)	14(1)	20(1)	4(1)
C(19)	38(1)	51(1)	79(1)	1`(1)	0(1)	-1(1)
C(20)	47(1)	48(1)	55(1)	2(1)	-4(1)	5(1)
C(21)	39(1)	45(1)	44(1)	5(1)	7(1)	8(1)

Table 9. Hydrogen coordinates (x 10^4) and isotropic displacement parameters (A^2 x 10^3) for **2b**.

	x	y	z	U(eq)
H(2A)	-99(1)	7551(2)	-593(1)	73
H(3A)	1600(1)	5960(2)	-118(1)	70
H(5A)	3268(1)	9435(2)	1509(1)	64
H(6A)	1561(1)	11021(2)	1039(1)	65
H(9A)	3794(1)	2057(2)	406(1)	56
H(10A)	5467(1)	398(2)	748(1)	64
H(11A)	7386(1)	1376(2)	1502(1)	64
H(12A)	7644(1)	4034(2)	1872(1)	58
H(15A)	4916(1)	8318(2)	1600(1)	46
H(17A)	7906(1)	6389(2)	983(1)	56
H(18A)	9712(1)	7832(2)	1465(1)	69
H(19A)	10023(1)	9519(2)	2673(1)	71
H(20A)	8519(1)	9790(2)	3398(1)	64
H(21A)	6722(1)	8347(2)	2933(1)	53